

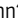
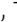










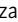





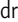
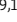


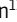
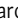
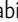

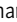


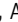




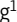










BRIEF DEFINITIVE REPORT

Auto-antibodies to type I IFNs can underlie adverse reactions to yellow fever live attenuated vaccine

Paul Bastard^{1,2,3} , Eleftherios Michailidis^{4*} , Hans-Heinrich Hoffmann^{4*} , Marwa Chbihi^{1,2*} , Tom Le Voyer^{1,2} , Jérémie Rosain^{1,2} , Quentin Philippot^{1,2} , Yoann Seeleuthner¹ , Adrian Gervais^{1,2} , Marie Materna^{1,2} , Patricia Mouta Nunes de Oliveira⁵ , Maria de Lourdes S. Maia⁵ , Ana Paula Dinis Ano Bom⁶ , Tamiris Azamor⁶ , Deborah Araújo da Conceição⁵ , Ekaterini Goudouris⁷ , Akira Homma⁵ , Günther Slesak⁸ , Johannes Schäfer⁸ , Bali Pulendran^{9,10} , Joseph D. Miller^{9,11} , Ralph Huits¹² , Rui Yang³ , Lindsey B. Rosen¹³ , Lucy Bizien^{1,2} , Lazaro Lorenzo^{1,2} , Maya Chrabieh^{1,2} , Lucia V. Erazo¹ , Flore Rozenberg¹⁴ , Mohamed Maxime Jeljeli¹⁵ , Vivien Béziat^{1,2,3} , Steven M. Holland¹³ , Aurélie Cobat^{1,3} , Luigi D. Notarangelo¹³ , Helen C. Su¹³ , Rafi Ahmed⁹ , Anne Puel^{1,2,3} , Shen-Ying Zhang^{1,2,3} , Laurent Abel^{1,2,3} , Stephen J. Seligman^{3,16**} , Qian Zhang^{3**} , Margaret R. MacDonald^{4***} , Emmanuelle Jouanguy^{1,2,3***} , Charles M. Rice^{4***} , and Jean-Laurent Casanova^{1,2,3,17***} 

Yellow fever virus (YFV) live attenuated vaccine can, in rare cases, cause life-threatening disease, typically in patients with no previous history of severe viral illness. Autosomal recessive (AR) complete IFNAR1 deficiency was reported in one 12-yr-old patient. Here, we studied seven other previously healthy patients aged 13 to 80 yr with unexplained life-threatening YFV vaccine-associated disease. One 13-yr-old patient had AR complete IFNAR2 deficiency. Three other patients vaccinated at the ages of 47, 57, and 64 yr had high titers of circulating auto-Abs against at least 14 of the 17 individual type I IFNs. These antibodies were recently shown to underlie at least 10% of cases of life-threatening COVID-19 pneumonia. The auto-Abs were neutralizing in vitro, blocking the protective effect of IFN- α 2 against YFV vaccine strains. AR IFNAR1 or IFNAR2 deficiency and neutralizing auto-Abs against type I IFNs thus accounted for more than half the cases of life-threatening YFV vaccine-associated disease studied here. Previously healthy subjects could be tested for both predispositions before anti-YFV vaccination.

Introduction

The 17D live attenuated vaccine against yellow fever virus (YFV) was approved for use in humans by the World Health Organization in 1945. It has since been used to vaccinate more than 600 million people worldwide, with very high rates of seroconversion following the administration of a single dose, providing long-term protection (Monath, 2005; Monath et al., 2005). About half the vaccine recipients develop transient low-level viremia detectable 4–6 d after inoculation, a timing similar to that for viremia after WT YFV infection. All live attenuated YFV

vaccines in current use are derivatives of the 17D strain and produced by amplification in embryonated chicken eggs. Although initially considered to be the world’s safest live virus vaccine, rare cases of life-threatening disease following vaccination with YFV-17D were subsequently detected from 2001 onward (Chan et al., 2001; Martin et al., 2001; Seligman, 2014; Vasconcelos et al., 2001). Systemic disease with clinical manifestations of organ dysfunction is often reported as yellow fever vaccine-associated viscerotropic disease (YEL-AVD; Seligman,

¹Laboratory of Human Genetics of Infectious Diseases, Necker Branch, Institut National de la Santé et de la Recherche Médicale U1163, Necker Hospital for Sick Children, Paris, France; ²University of Paris, Imagine Institute, Paris, France; ³St. Giles Laboratory of Human Genetics of Infectious Diseases, Rockefeller Branch, The Rockefeller University, New York, NY; ⁴Laboratory of Virology and Infectious Disease, The Rockefeller University, New York, NY; ⁵Bio-Manguinhos, Fiocruz, Ministry of Health, Rio de Janeiro, Brazil; ⁶Laboratory of Immunological Techniques, Bio-Manguinhos, Fiocruz, Ministry of Health, Rio de Janeiro, Brazil; ⁷Federal University of Rio de Janeiro, Rio de Janeiro, Brazil; ⁸Tropical Medicine Department, Tropenlinik Paul-Lechler-Krankenhaus, Tübingen, Germany; ⁹Emory Vaccine Center and the Department of Microbiology and Immunology, Emory University School of Medicine, Atlanta, GA; ¹⁰Institute for Immunity, Transplantation and Infection, Department of Pathology, Department of Microbiology and Immunology, Stanford University, Stanford, CA; ¹¹Centers for Disease Control and Prevention, National Center for Emerging and Zoonotic Infectious Diseases, Division of Scientific Resources, Atlanta, GA; ¹²Department of Clinical Sciences, Institute of Tropical Medicine, Antwerp, Belgium; ¹³Laboratory of Clinical Immunology and Microbiology, National Institute of Allergy and Infectious Diseases, National Institutes of Health, Bethesda, MD; ¹⁴Laboratory of Virology, University of Paris, Cochin Hospital, Assistance Publique–Hôpitaux de Paris, Paris, France; ¹⁵Laboratory of Immunology, University of Paris, Cochin Hospital, Assistance Publique–Hôpitaux de Paris, Paris, France; ¹⁶New York Medical College, Valhalla, NY; ¹⁷Howard Hughes Medical Institute, New York, NY.

*E. Michailidis, H.-H. Hoffmann, and M. Chbihi contributed equally to this paper; **S.J. Seligman and Q. Zhang contributed equally to this paper; ***M.R. MacDonald, E. Jouanguy, C.M. Rice, and J.-L. Casanova contributed equally to this paper; Correspondence to Paul Bastard: paul.bastard@institutimagine.org; Jean-Laurent Casanova: jean-laurent.casanova@rockefeller.edu.

© 2021 Bastard et al. This article is distributed under the terms of an Attribution–Noncommercial–Share Alike–No Mirror Sites license for the first six months after the publication date (see <http://www.rupress.org/terms/>). After six months it is available under a Creative Commons License (Attribution–Noncommercial–Share Alike 4.0 International license, as described at <https://creativecommons.org/licenses/by-nc-sa/4.0/>).

2014), and cases with neurological manifestations are referred to as yellow fever vaccine-associated neurological disease (YEL-AND). The prevalences of these conditions are ~ 0.3 and ~ 0.8 per 100,000 vaccinees, respectively (Lindsey et al., 2016). However, prevalence estimates vary, ranging, for YEL-AVD, from 0–0.01 per 100,000 vaccinees in Africa, to 0.02–0.31 per 100,000 vaccinees in Brazil, and 0.35 per 100,000 vaccinees in the United States, which is considered to be the most accurate estimate. The incidence of YEL-AND is estimated at 0.39 per 10^5 administered vaccine doses (range, 0.02–1.5; Lecomte et al., 2020). Mortality rates vary depending on age, but approximately two thirds of individuals die (Seligman, 2014). The rate of severe adverse events seems to increase with age, particularly after the age of 55 yr, and is higher in men (Lindsey et al., 2016; Seligman, 2014). Women in their prime child-bearing years and patients with thymoma are also at risk (Seligman, 2014). Severe adverse reactions have also occurred in association with various autoimmune diseases, including systemic lupus erythematosus (SLE), Addison's disease, pernicious anemia, and myasthenia gravis, suggesting an immunological mechanism (Martins et al., 2014; Seligman, 2014; Seligman and Casanova, 2016).

We provided an explanation for life-threatening disease following YFV-17D vaccination in 2019, with the discovery of autosomal recessive (AR), complete IFNAR1 deficiency in a 14-yr-old Brazilian girl with no prior history of severe viral illness who suffered from YEL-AVD (Hernandez et al., 2019). This study also highlighted the crucial role of type I IFNs in controlling live attenuated YFV-17D. Four other patients with IFNAR1 deficiency have been reported: a 9-yr-old child from Iran with measles-mumps-rubella (MMR) live vaccine-associated disease (Hernandez et al., 2019), a 2-yr-old child from Palestine with herpes simplex encephalitis (Bastard et al., 2020a), and two adults, aged 26 and 38 yr, from Saudi Arabia and Turkey, with life-threatening COVID-19 pneumonia (Zhang et al., 2020b). A case of YEL-AVD was also reported in a 1-yr-old patient with a suspected AR deficiency of IRF9, a component of the ISGF3 complex activated by both type I and III IFNs (Bravo García-Morato et al., 2019). Another child, with severe influenza pneumonia, had proven AR IRF9 deficiency but was not vaccinated against yellow fever (Hernandez et al., 2018). Thus, inborn errors of type I IFN immunity can underlie life-threatening disease following vaccination against YFV. We studied seven other unrelated and previously healthy patients, currently aged 35 to 80 yr, who had suffered from YEL-AVD ($n = 5$) and/or YEL-AND ($n = 3$; Table 1; Lecomte et al., 2020; Pulendran et al., 2008; Slesak et al., 2017). All had suffered life-threatening complications following vaccination with YFV-17D. In this report, we tested the hypothesis that some of these patients carry deleterious variants of genes of the type I IFN pathway, including *IFNAR2*, encoding the second chain of the type I IFN receptor (Duncan et al., 2015), *JAK1* and *TYK2*, encoding the two kinases constitutively associated with the receptors (Eletto et al., 2016; Kreins et al., 2015; Lazear et al., 2019; Russell-Harde et al., 2000; Wilmes et al., 2015), and *STAT1*, *STAT2*, and *IRF9*, encoding the three components of ISGF-3 (Dupuis et al., 2003; Hambleton et al., 2013; Hernandez et al.,

2018). We also tested the hypothesis that auto-antibodies (auto-Abs) against type I IFNs may be causal for disease, as recently reported in 10% of patients suffering from severe COVID-19 (Bastard et al., 2020b; Zhang et al., 2020a).

Results and discussion

A rare homozygous essential splice variant of *IFNAR2* in one patient

In addition to the patient with proven AR IFNAR1 deficiency (Hernandez et al., 2019), we studied seven patients who had experienced life-threatening disease following vaccination with the YFV-17D vaccine (Table 1). We performed whole-exome sequencing in all patients. Principal component analysis confirmed that the patients were of different ancestries (Fig. S1 A). We hypothesized that the patients developed YEL-AVD and/or YEL-AND because of monogenic inborn errors of immunity (IEIs) compromising the cellular response to type I IFNs (*IFNAR1*, *IFNAR2*, *STAT1*, *STAT2*, and *IRF9* genes; Bastard et al., 2020a; Duncan et al., 2015; Dupuis et al., 2003; Hambleton et al., 2013; Hernandez et al., 2019; Hernandez et al., 2018). We also considered possible defects of *JAK1* and *TYK2*, although both encode proteins that are much more pleiotropic than the components of the ISGF3 complex (Eletto et al., 2016; Kreins et al., 2015). We tested this hypothesis by searching for homozygous single-nucleotide variants or large deletions (copy number variants). We filtered out common variants (minor allele frequency [MAF] > 0.01) and variants predicted to be benign (combined annotation-dependent depletion score below the mutation significance cutoff within the 99% confidence interval; Itan et al., 2016; Kircher et al., 2014; Fig. S1 B). We also analyzed all genes underlying known IEIs (Bousfiha et al., 2020; Notarangelo et al., 2020; Tangye et al., 2020). We found that one patient (P1) carried a homozygous essential splicing variant of *IFNAR2* (c.840+1G>T). P1 is a 35-yr-old woman from Brazil who suffered from YEL-AVD at the age of 13 yr. She had no previous history of severe viral infections. 3 d after vaccination with YFV-17D, P1 presented with fever and digestive symptoms. She was admitted to the hospital 4 d later for epistaxis, hepatitis, and hypotension. She recovered with supportive care. Her sister died from YEL-AVD at the age of 19 yr, but no samples were available for this study (Fig. 1 A). There were no rare variants in the other six candidate genes or in known IEI genes. The patient's homozygosity rate was 0.88%, and there were only seven other homozygous rare nonsynonymous variants in her exome, none of which was connected to antiviral immunity (Fig. S1 C). The *IFNAR2* variant was confirmed by Sanger sequencing and was found to be present in the heterozygous state in both of P1's parents and in several other members of her family (Fig. 1 B). This variant was present in the gnomAD v3.1 public database but was extremely rare (MAF = 1.3×10^{-5}) and found only in the heterozygous state (Fig. S1 D). Given the crucial role of human *IFNAR2* in the type I IFN pathway (Duncan et al., 2015) and the previously described IFNAR1-deficient patient with YEL-AVD (Hernandez et al., 2019), we hypothesized that the homozygous essential splice site variant of *IFNAR2* might underlie the pathogenesis of the adverse reaction to YFV-17D in P1.

Table 1. Clinical and epidemiological characteristics of the eight patients included in the study with adverse events following YFV-17D vaccination

Case no.	Auto-Abs to type I IFNs	Inborn errors of type I IFNs ^a	Country of origin and residence	Sex	Age (yr)	Family history	YFV-17D disease	Vaccination year and age	Clinical and biological features	YFV-17D isolate	Other severe infectious diseases and age (yr)	Co-morbidities (age of diagnosis)	Patient
1	Negative	AR IFNAR1 deficiency	Brazil	F	16	—	YEL-AVD	2017, 12 yr	Fever, shock, renal and hepatic insufficiency, pleural effusion and atelectasis	Blood	No	None	P2, Hernandez et al., 2019
2	Negative	AR IFNAR2 deficiency	Brazil	F	35	Sister died from YEL-AVD at 19 yr	YEL-AVD	1999, 13 yr	Fever, hypotension, bleeding, hepatitis, thrombopenia	Not tested	No	None	P1, this report
3	Positive	Negative	Germany	M	62	—	YEL-AND/ YEL-AVD	2016, 57 yr	Fever, meningoencephalitis, hepatitis	Urine	Influenza B pneumonia, 59 yr	None	P2, this report
4	Positive	Negative	Brazil	F	50	—	YEL-AVD	2017, 47 yr	Fever, shock, renal insufficiency, hepatic insufficiency, thrombopenia	Blood	No	SLE (47 yr)	P3, this report
5	Positive	Negative	US	M	80	—	YEL-AVD	2004, 64 yr	Fever, shock, renal insufficiency, thrombopenia, hepatitis	Blood	No	None	P4, this report
6	Negative	Negative	Brazil	M	25	2 siblings (brother, aged 32 yr and sister, aged 32 yr) died from YEL-AVD	YEL-AVD	2018, 28 yr	Fever, nausea, vomiting, headache, hepatitis	Blood	No	None	—
7	Negative	Negative	Brazil	M	25	Father: myasthenia gravis	YEL-AND	2017, 22 yr	Fever, headache, vomiting, dizziness	CSF	No	None	—
8	Negative	Negative	Belgium	M	56	-	YEL-AND	2020, 56 yr	Fever, headache, cognitive problems	CSF	No	None	—

F, female; M, male.

^aCoding regions of IFNAR1, IFNAR2, TYK2, JAK1, STAT1, STAT2, and IRF9.

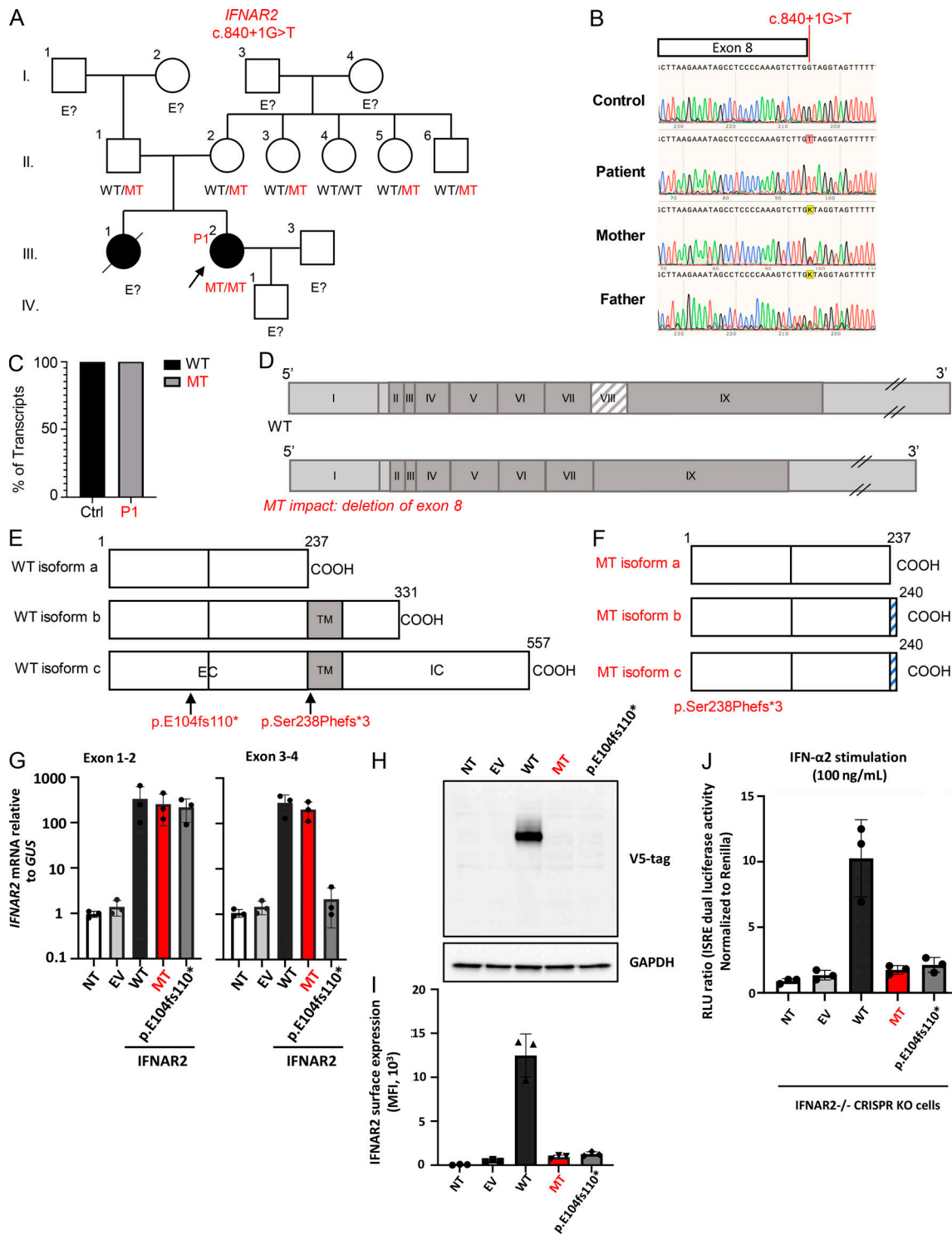


Figure 1. Homozygous loss-of-function variant of *IFNAR2* in a patient with YEL-AVD. (A) Family pedigree showing the segregation of the *IFNAR2* MT allele. The proband is indicated by an arrow. E?, unknown *IFNAR2* genotype. **(B)** Sanger sequencing results for *IFNAR2* for the patient, her parents, and healthy control leukocyte gDNA. **(C)** Exon trapping results demonstrating complete aberrant splicing in MT *IFNAR2*-transfected COS-7 cells. At least 100 transcripts were sequenced for the patient and the control. **(D)** Schematic diagram of the full-length cDNA of the WT or MT *IFNAR2*. The exons are numbered by roman numerals (I–IX). The 5' and 3' untranslated region is shown in light gray, and the coding sequences of the exons are shown in dark gray. **(E)** Schematic diagram of the WT *IFNAR2* proteins, with the three known isoforms. The transmembrane domain is denoted “TM.” EC, extracellular domain; IC, intracellular domain. The mutation reported here is indicated in red, and the previously reported mutation is indicated in violet. **(F)** Schematic diagram of the MT *IFNAR2* proteins, with the impact on the three known isoforms. The shaded blue area shows the three amino acids resulting from the frameshift. **(G)** *IFNAR2* mRNA levels, determined by RT-qPCR in HEK293T cells transiently transfected with WT or MT *IFNAR2* cDNA constructs; β glucuronidase (GUS) was used as an expression control. EV, empty vector; NT, nontransfected; p.E104fs110*, variant from the previously published *IFNAR2*^{-/-} patient. Error bars represent standard deviation. **(H)** Western blot of *IFNAR2* in HEK293T cells transiently transfected with *IFNAR2* isoform c cDNA constructs. An Ab recognizing the V5 tag at the C-terminal

end of the IFNAR2 protein was used. GAPDH was used as a loading control. A representative blot from two independent experiments is shown. (I) Graphical representation of extracellular FACS staining and the mean fluorescence intensity (MFI) of IFNAR2 in HEK293T cells transiently transfected with *IFNAR2* cDNA constructs, using an Ab that recognizes the N-terminus of the protein. Cells were not permeabilized. Results representative of three independent experiments are shown. Error bars represent standard deviation. (J) Luciferase activity after IFN- α 2 stimulation in *IFNAR2*^{-/-} HEK293T cells generated with CRISPR/Cas-9 technology, and transiently transfected with WT or MT *IFNAR2* cDNA constructs. Results shown are from three cell lines generated with three independent CRISPR guide RNAs. The bars represent the means and SEM of the results obtained with three cell lines generated with three different CRISPR guide RNAs. Each dot corresponds to the result obtained with one of these three cell lines. Ctrl, control; ISRE, interferon stimulation response element; RLU, relative light units.

AR complete IFNAR2 deficiency

The *IFNAR2* variant was predicted *in silico* to alter splicing and to lead to the loss of exon 8 (Fig. S1 E). We thus performed exon trapping on the patient's genomic DNA (gDNA) to test the impact of the variant. As predicted, a complete loss of exon 8 was observed in analyses of mRNA from the patient but not in analyses of mRNA from a healthy control (Fig. 1, C and D; and Fig. S1 F). We also performed mutagenesis on gDNA to restore the patient's variant to the WT form, which restored normal splicing (Fig. S1 G). Human IFNAR2 is a ubiquitously expressed transmembrane protein that constitutively binds JAK1 (Russell-Harde et al., 2000; Wilmes et al., 2015). The loss of exon 8 is predicted to lead to a frameshift and a premature stop codon (p.Ser238Phefs*3; Fig. 1, E and F). We first studied the expression of the mutant (MT) IFNAR2 by plasmid-mediated overexpression in HEK293T cells. Following the transient transfection of cells with plasmids containing the WT or MT *IFNAR2* cDNA (isoform c), similar levels of *IFNAR2* mRNA were detected for the WT, MT, and previously published variant (p.E104fs110*) when using a probe spanning exons 1 and 2 (Fig. 1 G). Western blot analysis of these cell extracts with a C-terminal tag showed the protein to be absent, consistent with the loss of exon 8 leading to a frameshift without translation reinitiation (Fig. 1 H). We then performed flow cytometry to analyze the cell surface expression of WT and MT IFNAR2 in transfected HEK293T cells. The MT protein was not detected on the cell surface (Fig. 1 I). Finally, we used the WT or MT *IFNAR2* cDNA to transfect IFNAR2 KO HEK293T cells, which we created by CRISPR/Cas9-mediated gene editing. Upon stimulation with IFN- α 2 and transfection with a reporter gene, the cells expressing WT IFNAR2 displayed luciferase activity, unlike those expressing MT IFNAR2 (Fig. 1 J). We did not test the response of the patient's cells to type I IFNs, but previous reports have indicated that the fibroblasts from patients with IFNAR2 deficiency are unresponsive to IFN- α 2 and IFN- β (Bastard et al., 2020a; Duncan et al., 2015). P1 had AR complete IFNAR2 deficiency. Together with our previous report of a patient with AR IFNAR1 deficiency underlying YEL-AVD (Hernandez et al., 2019), these findings show that two of the eight patients in our cohort with severe adverse reactions to YFV-17D vaccination had an AR complete deficiency of one of the chains of the type I IFN receptor. They were surprisingly healthy before vaccination with YFV-17D at 12 and 13 yr of age.

Auto-Abs against IFN- α 2 and IFN- ω in three unrelated patients

No nonsynonymous variants of *IFNAR1*, *IFNAR2*, or the five genes controlling the type I IFN response pathway (*JAK1*, *TYK2*, *STAT1*, *STAT2*, and *IRF9*; Bastard et al., 2020a; Dupuis et al., 2003;

Eletto et al., 2016; Gothe et al., 2020; Hambleton et al., 2013; Hernandez et al., 2018; Kreins et al., 2015; Watford and O'Shea, 2006) were found in the other six patients. We then hypothesized that these patients might have an autoimmune phenocopy of inborn errors of type I IFN immunity, as recently shown in patients with life-threatening COVID-19 pneumonia (Bastard et al., 2020b; Ku et al., 2020; Zhang et al., 2020a; Zhang et al., 2020b). We therefore searched for IgG auto-Abs against IFN- α 2 and IFN- ω by ELISA and with a Luminex assay. We found high titers in three (P2, P3, and P4) of the six patients tested (Fig. 2 A and Fig. S2 A). P2 is a 62-yr-old man originating from and living in Germany, with no prior history of severe viral infections. At the age of 57 yr, 5 d after YFV-17D vaccination, before traveling to Zanzibar, he developed neurological symptoms consistent with YEL-AND, and his liver enzyme levels increased (Slesak et al., 2017). He was also hospitalized 2 yr later, at the age of 59 yr, for influenza B infection with bilateral interstitial pneumonia. The blood sample positive for auto-Abs against type I IFNs was taken 6 mo after YFV-17D disease. P3 is a 50-yr-old Brazilian woman with no history of severe viral infections. She presented with YEL-AVD following YFV-17D vaccination at the age of 47 yr. 3 d after vaccination, she reported fever, headache, and myalgia, which rapidly worsened. She was subsequently admitted to the hospital with shock, acute renal and hepatic insufficiency, and thrombopenia. She was hospitalized in the intensive care unit for 2 mo. Of note, she reported a history of 3 mo of polyarthralgia before hospitalization, and a history of miscarriage and preterm birth for her two pregnancies. She was diagnosed with SLE during her hospital stay. Not coincidentally, women with SLE have been reported to be both at risk of adverse reactions to YFV-17D vaccination (Seligman, 2014) and prone to producing auto-Abs against type I IFN (Gupta et al., 2016; Howe and Leung, 2019; Mathian et al., 2019; Panem et al., 1982). The blood sample positive for auto-Abs against type I IFNs was taken when the patient was 49 yr old, 2 yr after YFV-17D disease. P4 is an 80-yr-old man originating from and living in the United States, with no prior history of severe viral infections. At the age of 64 yr, 2 d after YFV-17D vaccination, he developed fever and digestive symptoms. His condition quickly deteriorated, and he was hospitalized 2 d later for hypotension, skin rash, high fever, renal insufficiency, cytolysis, and thrombopenia (Pulendran et al., 2008). The blood sample positive for auto-Abs was taken 16 d after the onset of YFV-17D disease. Interestingly, all patients tested (including P2 and P3) had been exposed to several common viruses (Fig. S2 B), and P2 and P3 were positive for anti-nuclear auto-Abs (Table S1). Three of the eight patients with adverse reactions to YFV vaccination studied therefore had high titers of auto-Abs to type I IFNs.

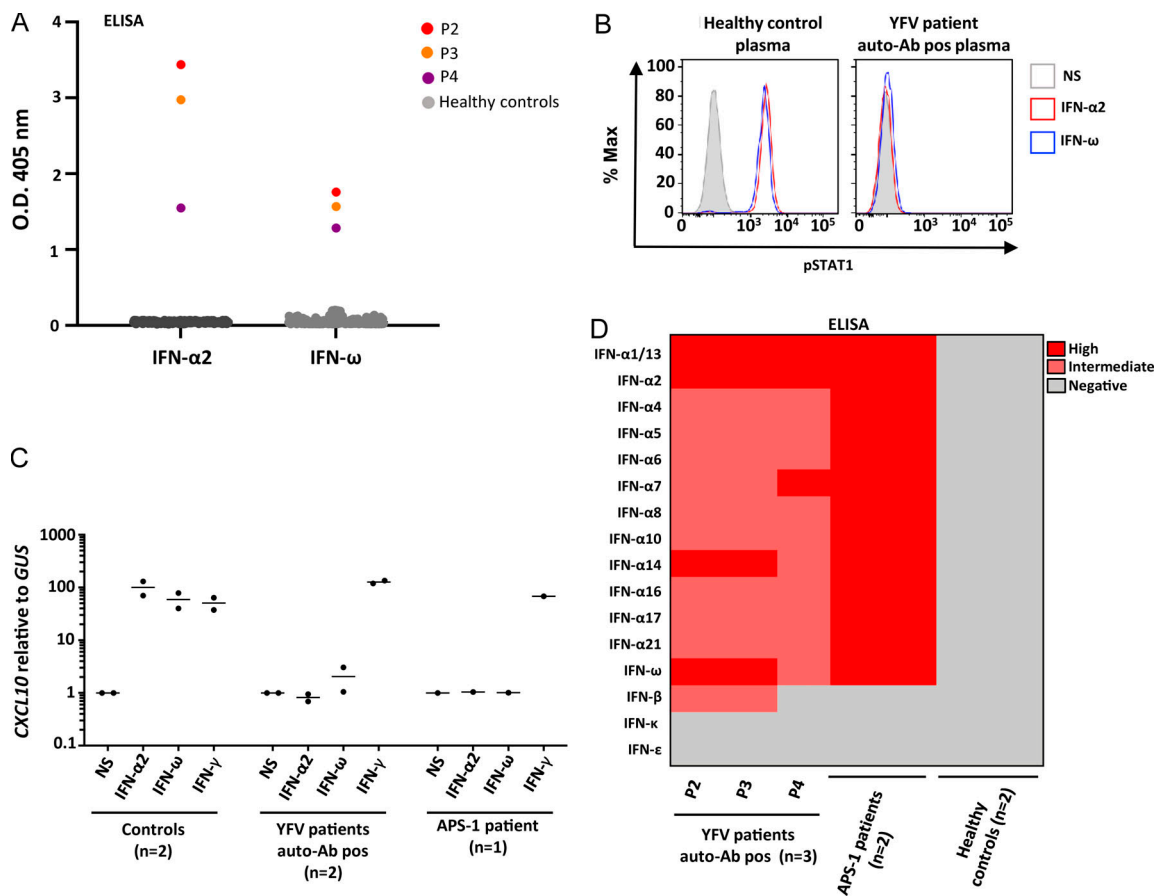


Figure 2. Neutralizing auto-Abs against IFN-α2 and IFN-ω in three patients with adverse reactions to yellow fever vaccine. (A) ELISA assay for auto-Abs against IFN-α2 and IFN-ω in three patients with life-threatening adverse reactions to yellow fever vaccine and healthy controls ($n = 200$). **(B)** Representative flow cytometry plots for IFN-α2- or IFN-ω-induced pSTAT1 in healthy control cells (gated on CD14⁺ monocytes) in the presence of 10% healthy control plasma or anti-IFN-α2, or anti-IFN-ω auto-Ab-containing plasma from patients. Max, maximum; pos, positive; NS, not stimulated. **(C)** Neutralization effect on CXCL10 induction relative to GUS after the stimulation of healthy control PBMCs with IFN-α2, IFN-ω, or IFN-γ, in the presence of plasma from either healthy controls ($n = 2$), two patients with adverse reactions to yellow fever vaccine and auto-Abs (P2 and P3), or one APS-1 patient. **(D)** Auto-Abs against the different type I IFN subtypes. ELISA for auto-Abs against the 13 different IFN-α subtypes, IFN-ω, IFN-β, IFN-κ, and IFN-ε in the three patients with adverse reactions to yellow fever vaccine and auto-Abs against IFN-α2, APS-1 patients ($n = 2$), and healthy controls ($n = 2$).

The auto-Abs are neutralizing and recognize most of the 17 subtypes of type I IFN

We then investigated whether these auto-Abs were neutralizing *in vitro* (i.e., if they could block the activity of recombinant type I IFNs in an experimental assay). We incubated peripheral blood mononuclear cells (PBMCs) derived from a healthy control individual with 10% plasma from a healthy control or from the three patients, and stimulated the cells with IFN-α2 or IFN-ω. We found that the presence of plasma from the three patients completely abolished type I IFN signaling, as shown by analyses of pSTAT1 induction following treatment with IFN-α2 or IFN-ω (Fig. 2 B and Fig. S2 C). For P2 and P3, we also analyzed the induction of IFN-stimulated genes after 2 h of stimulation with IFN-α2 or IFN-ω, using type II IFN (IFN-γ) as a control. The incubation of cells with plasma from either patient led to the abolition of IFN-stimulated gene induction in response to either of the individual type I IFNs tested, but not in response to type II IFN. By contrast, induction in response to both type I and II IFNs

remained normal in the presence of plasma from healthy control individuals (Fig. 2 C). We tested the three patients for auto-Abs against the other 15 individual type I IFNs by performing ELISA with recombinant proteins for the 17 individual type I IFNs. We found that P2, P3, and P4 had auto-Abs recognizing at least 14 subtypes (Fig. 2 D), a finding similar to that for most of the patients with life-threatening COVID-19 carrying auto-Abs against type I IFNs and autoimmune polyendocrine syndrome type 1 (APS-1; Bastard et al., 2020b), although two patients (P2 and P3) also had neutralizing auto-Abs against IFN-β (Fig. S2 C). The plasma samples from P2, P3, and P4 did not recognize IFN-κ or IFN-ε, at least in the experimental conditions tested. These two type I IFNs were not, however, sufficient to protect the patients from YFV-17D infection. Overall, we found that three patients presenting severe adverse reactions to YFV-17D vaccination had high titers of neutralizing auto-Abs against type I IFNs and that these auto-Abs recognized most of the 17 individual type I IFN subtypes.

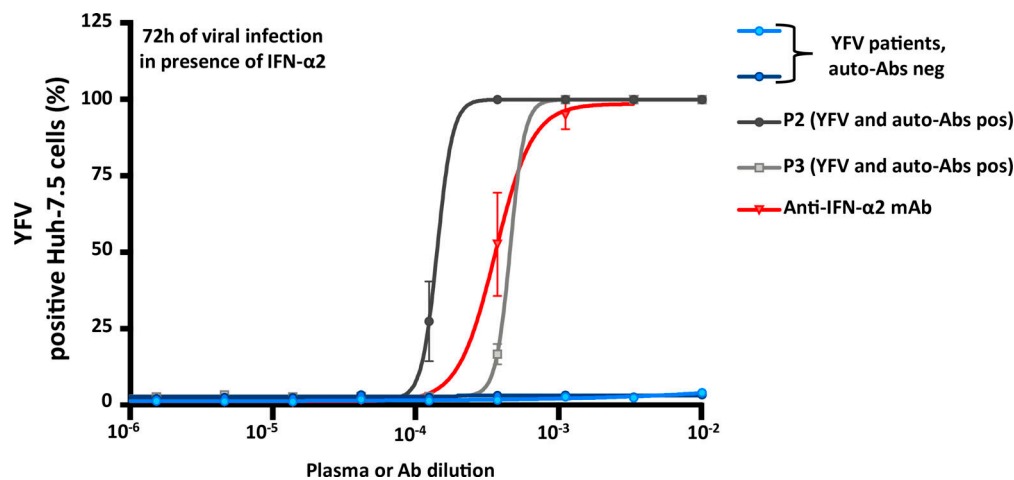


Figure 3. **Enhanced YFV replication, despite the presence of IFN- α 2, in the presence of plasma from patients with auto-Abs against IFN- α 2.** YFV-17D replication, assessed 72 h after infection, in Huh-7.5 cells treated with IFN- α 2 in the presence of plasma from either patients with life-threatening adverse reactions to YFV and neutralizing auto-Abs against IFN- α 2 ($n = 2$, P2 and P3), or a commercial anti-IFN- α 2 Ab, or plasma from patients with adverse events following YFV vaccination but without auto-Abs against type I IFNs ($n = 2$). Error bars represent SEM. neg, negative; pos, positive.

The auto-Abs neutralize IFN- α 2-mediated protection against YFV-17D in vitro

Finally, we investigated whether these auto-Abs blocking type I IFN in biochemical assays were also able to block type I IFN-mediated protection against YFV-17D infection in cells in vitro. Plasma from P2 and P3, who had auto-Abs against type I IFNs, clearly blocked the ability of IFN- α 2 to protect Huh-7.5 cells from infection with YFV-17D (Fig. 3). By contrast, plasma from two healthy donors without auto-Abs or from two other patients with severe YFV infection but without auto-Abs did not block the protective effect of IFN- α 2 (Fig. 3). Furthermore, plasma from eight previously reported patients with life-threatening COVID-19 and auto-Abs against IFN- α 2 also blocked the protective effect of IFN- α 2 against YFV-17D (Fig. S3), in addition to that against SARS-CoV-2 (Bastard et al., 2020b). Interestingly, the three patients reported here belong to two groups known to be at higher risk of displaying auto-Abs against type I IFNs: P2 and P4 are men over the age of 55 yr (Bastard et al., 2020b; Seligman, 2014), and P3 is a 47-yr-old woman with SLE (Panem et al., 1982). Finally, we found that the prevalence of auto-Abs against type I IFNs in our cohort of patients with severe adverse events following YFV-17D vaccination and without known IEI was significantly higher than the estimated prevalence in the general population (Bastard et al., 2020b; 37.5% vs. 0.3%; Fisher's exact test, $P = 6.2 \times 10^{-6}$). It is also probably not coincidental that the two patients with inherited IFNAR1 and IFNAR2 deficiency were younger, at 12 and 13 yr, and did not display auto-Abs against type I IFNs. This suggests that the two mechanisms disrupting type I IFN immunity and resulting in YFV-17D disease are related but independent. This finding is reminiscent of our recent reports of inborn errors of type I IFNs and auto-Abs against type I IFNs in nonoverlapping groups of patients with life-threatening COVID-19 pneumonia (Bastard et al., 2020b; Zhang et al., 2020a; Zhang et al., 2020b). Overall, these findings strongly suggest that the three patients reported here suffered adverse reactions to YFV-17D because of preexisting neutralizing

auto-Abs against type I IFNs, which targeted most of the individual subtypes of type I IFN, blocking their protective effect against YFV-17D.

Impaired type I IFN immunity underlies yellow fever vaccine adverse events

Two members of our cohort of eight patients with YEL-AVD or YEL-AND have AR IFNAR1 or IFNAR2 deficiency, and another three have neutralizing auto-Abs against type I IFNs. These results suggest that at least half the patients with severe adverse reactions to YFV-17D have inadequate type I IFN immunity. This may be the case for the 78 reported patients with YEL-AVD or YEL-AND, including our five patients (Martins et al., 2014; Hernandez et al., 2019; Lindsey et al., 2016; Seligman, 2014; Seligman and Casanova, 2016; Slesak et al., 2017). These findings unambiguously place human type I IFNs at the core of protective immunity to YFV-17D. They have important clinical implications. First, patients with known inborn errors of, or auto-Abs against, type I IFN should not be vaccinated with YFV-17D. Second, patients with adverse reactions to YFV-17D should be tested for inborn errors of type I IFN immunity and for the presence of auto-Abs against type I IFNs. Third, both types of patients may benefit from treatment with recombinant IFN- β in the course of YFV-17D disease, provided that they do not have auto-Abs against IFN- β (such Abs were present in two of the three patients reported here but were absent from 99 of 101 patients from a previous report on severe COVID-19; Bastard et al., 2020b). Fourth, patients with autoimmune manifestations, including SLE and thymoma in particular, should be screened for auto-Abs against type I IFNs before vaccination with YFV-17D, as, perhaps, should men over the age of 55 yr. Younger patients may nevertheless also be at risk of adverse reactions to YFV-17D vaccination due to preexisting auto-Abs against type I IFNs, as suggested by the case of an 8-yr-old patient homozygous for a hypomorphic RAG1 mutation who had defective adaptive immunity, multiple severe infectious

diseases, auto-Abs against type I IFNs, and encephalitis after YFV-17D vaccination (Walter et al., 2015; Table S1, JCI80477sdt1). Moreover, the youngest patient with life-threatening COVID-19 pneumonia and auto-Abs against type I IFNs reported to date was 25 yr old (Bastard et al., 2020b), younger than the two patients with inherited IFNAR1 deficiency and critical COVID-19, aged 26 and 38 yr (Zhang et al., 2020b). Although difficult in some regions, screening for both inborn errors of type I IFN immunity and auto-Abs against type I IFNs could, therefore, be considered for patients of all ages before vaccination with YFV-17D. Moreover, patients with auto-Abs against type I IFNs are likely to be at risk of developing an adverse event if vaccinated with the newly developed vaccine against SARS-CoV-2 that uses the YFV live attenuated vaccine as a carrier (Sanchez-Felipe et al., 2020).

Pre-existing auto-Abs against type I IFNs can underlie different viral diseases

Our findings also have implications for the pathogenic role of auto-Abs against type I IFNs. Our previous study on life-threatening COVID-19 suggested that the auto-Abs against type I IFNs were causal of disease, rather than triggered by SARS-CoV-2 (Bastard et al., 2020b). Indeed, they were already present in blood samples from 2 of the 101 patients, 95 of whom were men, collected before the onset of COVID-19. Moreover, they were detected early in the course of SARS-CoV-2 infection in the other patients, making it highly unlikely that these auto-Abs of the IgG type with a high affinity for type I IFNs were triggered by infection. Finally, these Abs are common in patients with two genetic diseases underlying severe COVID-19: APS-1 (Meager et al., 2006) and incontinentia pigmenti (Bastard et al., 2020b). The three patients with auto-Abs reported here add weight to this conclusion. Indeed, they developed YFV-17D disease within 5 d of vaccination. We did not test their blood for the presence of auto-Abs before vaccination, or even during YFV-17D disease, but the presence of these Abs 6 mo (P2), 2 yr (P3), and 16 d (P4) later provides compelling evidence for an association with disease (Fisher's exact test, $P = 6.2 \times 10^{-6}$), even without taking into account a previously reported patient whose YFV-17D disease may have been triggered by her many profound deficits of adaptive immunity other than auto-Abs against type I IFNs (Walter et al., 2015). Assuming that the three patients had auto-Abs at the time of hospital admission for YFV-17D disease, it would have been almost impossible for them to mount a neutralizing IgG response against a self-antigen so quickly. Furthermore, one of the patients (P3) was diagnosed with SLE during hospitalization, and her SLE symptoms began 3 mo before admission, consistent with the occurrence of such auto-Abs, as reported in ~5–10% of patients with SLE (Gupta et al., 2016; Mathian et al., 2019; Panem et al., 1982). The sex of the patient and age at the time of vaccination are similar to those in the other three known cases of SLE with YFV-17D disease (Seligman, 2014). Auto-Abs against type I IFNs can therefore underlie severe COVID-19 or YFV-17D disease. Intriguingly, children with APS-1 and auto-Abs to type I IFNs have been vaccinated with MMR without any reported adverse reaction, despite the occurrence of MMR disease in several patients with

inherited IFNAR1 or IFNAR2 deficiency (Bastard et al., 2020a; Duncan et al., 2015; Gothe et al., 2020; Hernandez et al., 2019). This may be due to the activity of IFN- β , IFN- κ , or IFN- ϵ in APS-1 patients, whose auto-Abs typically neutralize the 13 individual IFN- α 2 and IFN- ω (Bastard et al., 2020b; Meager et al., 2006). It is nevertheless tempting to speculate that other severe, unexplained viral illnesses, such as shingles and influenza, particularly but not exclusively, in patients with autoimmune conditions or in elderly men, may be caused by auto-Abs against type I IFNs.

Materials and methods

Patients and study approval

All cases of YEL-AVD and YEL-AND satisfied the Brighton Collaboration criteria (Gershman et al., 2012). The Brazilian patients were recruited by a collaboration with BioManguinhos/Fiocruz, as indicated in the acknowledgments. Additional patients were found from listings on ProMED (<https://promedmail.org>) and PubMed (<https://pubmed.ncbi.nlm.nih.gov/>). Written informed consent was obtained from patients in the country in which they were followed, in accordance with local regulations, and the study was approved by the institutional review boards of The Rockefeller University and Institut National de la Santé et de la Recherche Médicale. Experiments were conducted in the United States and France, in accordance with local regulations and with the approval of the institutional review boards of The Rockefeller University and Institut National de la Santé et de la Recherche Médicale, respectively.

Whole-exome sequencing

Exome capture was performed with the SureSelect Human All Exon 50 Mb kit (Agilent Technologies). Paired-end sequencing was performed on a HiSeq 2000 (Illumina) generating 100-base reads. We aligned the sequences with the GRCh37 reference build of the human genome with the Burrows-Wheeler transform (Li and Durbin, 2009). Downstream processing and variant calling were performed with the Genome Analysis Toolkit, SAMtools, and Picard (Li et al., 2009; McKenna et al., 2010). Substitution and InDel calls were made with the GATK Unified Genotyper. All variants were annotated with an annotation software system developed in house (Adzhubei et al., 2010; Kircher et al., 2014; Ng and Henikoff, 2001). The patients reported here did not consent to the deposition of their genomic data.

Statistical analysis

Comparisons of proportions were performed using a Fisher's exact test, as implemented in R (<https://cran.r-project.org/>). Principal component analysis was performed with Plink v1.9 software on whole-exome and whole-genome sequencing data with the 1000 Genomes Project phase 3 public database as a reference.

Cells

PBMCs were isolated by Ficoll-Paque density gradient (GE Life Science) centrifugation. Primary fibroblasts, SV40-immortalized

dermal fibroblasts, HEK293T kidney epithelial cells (*Homo sapiens*), VeroE6 kidney epithelial cells (*Chlorocebus sabaeus*), and Huh-7.5 hepatoma cells (*H. sapiens*) were maintained in DMEM (Thermo Fisher Scientific) supplemented with 10% FBS at 37°C under an atmosphere containing 5% CO₂. EBV-B cells were maintained in Roswell Park Memorial Institute medium (Thermo Fisher Scientific) supplemented with 10% FBS. All cells tested negative for mycoplasma contamination.

Exon trapping

DNA segments encompassing the *IFNAR2* exon 8 region were amplified from genomic DNA and inserted into the pSPL3 vector, between the *EcoRI* and *BamHI* sites. WT, MT (*IFNAR2* c.840+1G>T), or mutagenesis rescue plasmids were used to transfect COS-7 cells. After 24 h, total RNA was extracted and reverse-transcribed. The *IFNAR2* splicing products were amplified with flanking HIV-TAT sequences from the pSPL3 vector and ligated into the pCR4-TOPO vector (Invitrogen). Stellar cells (Takara) were transformed with the resulting plasmids. Colony PCR and sequencing with primers binding to the flanking HIV-TAT sequences of pSPL3 were performed to determine the splicing products produced by the WT and mutated alleles.

Plasmids

A plasmid containing the cDNA of *IFNAR2* was used (generously provided by Sandra Pellegrini, Pasteur Institute, Paris, France), and site-directed mutagenesis was performed to obtain the indicated MT constructs.

IFNAR2 overexpression by plasmid transfection and the generation of stably reconstituted cell lines

The *IFNAR2* plasmid was used to transfect HEK293T cells by incubation for 48 h in the presence of X-tremeGene 9 transfection reagent (Sigma-Aldrich). We used 1 µg of plasmid to transfect 0.5 × 10⁶ cells.

Western blotting

HEK293T cells were transfected for 36 h with WT or MT *IFNAR2*. Cells were lysed in NP-40 lysis buffer (280 mM NaCl, 50 mM Tris, pH 8, 0.2 mM EDTA, 2 mM EGTA, 10% glycerol, and 0.5% NP-40) supplemented with 1 mM dithiothreitol, PhosSTOP (Roche), and complete protease inhibitor cocktail (Roche). The protein lysate was subjected to SDS-PAGE, and the bands obtained were transferred to a nitrocellulose membrane. For detection of the protein overproduced following transfection, we used an HRP-conjugated anti-V5 Ab purchased from commercial suppliers. An anti-GAPDH (Santa Cruz) Ab was used as a loading control. The membrane was incubated overnight at 4°C with the primary Abs. SuperSignal West Pico chemiluminescent substrate (Thermo Fisher Scientific) was used to visualize HRP activity after incubation with secondary Abs, and this signal was detected with an Amersham Imager 600 (GE Life Sciences).

Flow cytometry

The cell surface expression of *IFNAR2* was assessed with a PE-conjugated mouse anti-*IFNAR2* (21385-3PBL; Assay Science) Ab. Cells were stained and then washed twice with PBS and analyzed

by flow cytometry. Data were acquired on a Gallios flow cytometer.

Generation of *IFNAR2*-deficient HEK293T cells

IFNAR2-deficient HEK293T cells were generated with the CRISPR/Cas9 system. Guide RNAs were designed with the Benchling design tool and inserted into lentiCRISPR v2, which was a gift from Feng Zhang (Broad Institute, Cambridge, MA; plasmid 52961; Addgene). The three guide RNAs were designed to bind and cut at different places in the *IFNAR2* gene, one in exon 3 (forward: 5'-CACCGCATATGAAATACCAAACACG-3'; reverse: 5'-AAACCGTGTGGTATTTCATATGC-3'), one in exon 4 (forward: 5'-CACCGCATTGCTGTATACAATCATG-3'; reverse: 5'-AAACCATGATTGTATACAGCAATGC-3'), and one in exon 5 (forward: 5'-CACCGTGAGTGGAGAAGCACACACG-3'; reverse: 5'-AAACCGTGTGTGCTTCTCCACTCAC-3'). Using X-tremeGENE 9 DNA Transfection Reagent (Roche), we transiently transfected WT HEK293T cells with the resulting plasmids and cultured them for 7 d before sorting *IFNAR2*-deficient cells by flow cytometry after staining with an Ab against *IFNAR2* (REA124; Miltenyi Biotec). The three resulting cell lines were subsequently tested to check for a lack of *IFNAR2* expression at the cell surface and were used in the luciferase assays.

Luciferase reporter assays

IFNAR2^{-/-} HEK293T cells generated by the CRISPR/Cas9 system were transfected with the indicated expression plasmids, firefly luciferase plasmids under the control of WT or MT *IFNAR2*, or human *ISRE* promoters in the pGL4.45 backbone, and a constitutively expressing *Renilla* luciferase plasmid for normalization (pRL-SV40). Cells were transfected in the presence of the X-tremeGene 9 transfection reagent (Sigma-Aldrich) for 36 h. Luciferase levels were measured with the Dual-Glo reagent, according to the manufacturer's protocol (Promega). Firefly luciferase values were normalized against *Renilla* luciferase values, and fold induction is shown relative to controls transfected with empty plasmids.

Quantitative RT-PCR (RT-qPCR)

RNA was isolated from PBMCs or from plasmid-transfected or untransfected HEK293T cells with a kit according to the manufacturer's protocol (Zymo Research), and treated with DNase (Zymo Research). RT was performed with random hexamers and the Superscript III reverse-strand synthesis kit according to the manufacturer's instructions (Thermo Fisher Scientific). RT-qPCR was performed with Applied Biosystems *Taqman* assays for *IFNAR2* and the β glucuronidase housekeeping gene for normalization. Results are expressed according to the ΔΔCt method, as described by the kit manufacturer.

Detection of anti-cytokine auto-Abs in a multiplex particle-based assay

Serum/plasma samples were screened for auto-Abs against IFN-α₂ and IFN-ω targets in a multiplex particle-based assay, in which magnetic beads with differential fluorescence were covalently coupled to recombinant human proteins (2.5 µg/reaction). Beads were combined and incubated with 1:100 diluted

serum/plasma samples for 30 min. Each sample was tested once. The beads were then washed and incubated with PE-labeled goat anti-human IgG (1 µg/ml) for 30 min. They were washed again and used in a multiplex assay run on a BioPlex X200 instrument. Patients with a fluorescence intensity >1,500 for IFN- α 2 or IFN- β or >1,000 for IFN- ω were tested for blocking activity.

ELISAs for anti-cytokine auto-Abs

ELISA was performed as previously described (Bastard et al., 2020b). In brief, 96-well ELISA plates (MaxiSorp; Thermo Fisher Scientific) were coated by incubation overnight at 4°C with 2 µg/ml rhIFN- α and rhIFN- ω (R&D Systems). Plates were then washed (PBS/0.005% Tween), blocked by incubation with 5% nonfat milk powder in the same buffer, washed again, and incubated with 1:50 dilutions of plasma from the patients or controls for 2 h at room temperature (or with specific mAbs as positive controls). Each sample was tested once. Plates were thoroughly washed. HRP-conjugated Fc-specific (Fc, fragment crystallizable region) IgG fractions from polyclonal goat antiserum against human IgG or IgA (Nordic Immunological Laboratories) were added to a final concentration of 2 µg/ml. Plates were incubated for 1 h at room temperature and washed. Substrate was added, and the OD was measured. A similar protocol was used to test for Abs against 12 subtypes of IFN- α , except that the plates were coated with cytokines from PBL Assay Science (11002-1).

Clinical screening for other auto-Abs

The assay for antinuclear Ab (ANA) was performed using an indirect immunofluorescence on Hep-2 cells (Novalite 704320; Inova Diagnostics, distributed by Werfen). Dilutions of 1:80 were performed with PBS for the screening test. In brief, 30 µl of each diluted serum was incubated in one well with fixed Hep-2 cells. After the cells were incubated and washed, they were incubated with DAPI-IgG-conjugated Abs. The results were analyzed using a Nikon Eclipse fluorescence microscope with a magnification 400 \times . Extractable nuclear antigen Abs were detected by ELISA (RNP, Sm, SSA/Ro, SSB/la, Scl70, and JO-1) using the ANA 8 Screen Kit (Euroimmun). Immunoblotting was performed for a larger extractable nuclear antigen panel detection (RNP, Sm, SSA/Ro, SSA/Ro 52 kD, SSB/la, Scl70, JO-1, centromere B, PCNA, nucleosome, histones, ribosomes P, type 2 mitochondria, and DFS 70) using the ANA Profil 3 Dot (Euroimmun). Anti-native DNA detection was performed by indirect immunofluorescence on the flagellate organism *Crithidia luciliae* using the KIT Theradiag and ELISA for Ab quantification using the anti-double-stranded DNA IgG KIT on ETI-MAX 3000 Equipment from Diasorin.

Functional evaluation of anti-cytokine auto-Abs

The blocking activity of anti-IFN- α and anti-IFN- ω auto-Abs was determined by assessing STAT1 phosphorylation in healthy control cells following stimulation with the appropriate cytokines in the presence of 10% serum/plasma from a healthy control or a patient. Surface-stained healthy control PBMCs (350,000/reaction) were cultured in serum-free Roswell Park Memorial Institute medium supplemented with 10% healthy

control or patient serum/plasma and were either left unstimulated or stimulated with IFN- α or IFN- ω (10 ng/ml) for 15 min at 37°C. Each sample was tested once. Cells were fixed, permeabilized, and stained for intranuclear phospho-STAT1 (Y701). Cells were acquired on a BD LSRFortessa cytometer with gating on CD14⁺ monocytes and analyzed with FlowJo software.

YFV-17D experiment

The generation of virus stocks for the YFV-17D reporter virus expressing the Venus fluorescent protein (YFV-Venus; derived from YF17D-5'G25Venus2AUbi) has been described elsewhere (Yi et al., 2011). Virus stock titers were determined by standard plaque assays on Huh-7.5 cells. YFV-Venus experiments were performed as follows: Huh-7.5 cells were used to seed 96-well plates at a density of 5×10^3 cells/well, with triplicate wells for each sample. The following day, serial threefold dilutions of plasma samples or a commercial anti-IFN- α 2 Ab (21100-1; R&D Systems) were incubated with 20 pM recombinant IFN- α 2 (11101-2; R&D Systems) for 1 h at 37°C (starting dilution: plasma samples = 1/100 and anti-IFN- α 2 Ab = 1/1,000). Following this incubation period, the cell culture medium was removed from the wells of the 96-well plate by aspiration and replaced with the plasma/Ab-IFN- α 2 mixture. The plates were incubated overnight, the plasma/Ab-IFN- α 2 mixture was removed, and the plates were washed with PBS to remove any anti-YFV-neutralizing Abs present. Fresh medium was then added to the wells. Cells were then infected with YFV-Venus at a multiplicity of infection of 0.05 PFU/cell, by directly dispensing the inoculum in the wells. After 3 d, the cells were fixed in formaldehyde, stained with DAPI, and imaged and analyzed as previously described (Bastard et al., 2020b).

Online supplemental material

Fig. S1 provides additional data on the homozygous loss-of-function variant of *IFNAR2* in a patient with YEL-AVD. Fig. S2 provides additional data on the neutralizing auto-Abs against IFN- α 2 and IFN- ω in three patients with adverse reactions to yellow fever vaccine. Fig. S3 shows enhanced YFV replication, despite the presence of IFN- α 2, in the presence of plasma from patients with life-threatening COVID-19 and auto-Abs against IFN- α 2. Table S1 contains data on auto-Abs against other targets, used in clinical practice in two patients positive for auto-Abs against type I IFNs (P2 and P3).

Acknowledgments

We thank the patients and their families for placing their trust in us. We warmly thank Y. Nemirovskaya, D. Papandrea, M. Woollet, D. Liu, S. Boucherit, C. Rivalain, and C. Patissier for administrative assistance. We warmly thank S. Meyer and A.-L. Neehus for their German translation. We thank S. Pellegrini and Z. Li for providing the *IFNAR2* plasmids. We thank the Imagine sequencing platform for all their help and understanding. We thank Stephen J. Seligman for initiating the recruitment of all the patients and for establishing a collaboration with the late Reinaldo de Menezes Martins, resulting in the inclusion of the Brazilian patients.

The Laboratory of Human Genetics of Infectious Diseases is supported by the Howard Hughes Medical Institute, The Rockefeller University, the St. Giles Foundation, the National Institutes of Health (R01AI088364), the National Center for Advancing Translational Sciences, the National Institutes of Health Clinical and Translational Science Award program (UL1TR001866), a Fast Grant from Emergent Ventures, the Mercatus Center at George Mason University, the Yale Center for Mendelian Genomics, the Genome Sequencing Program Coordinating Center funded by the National Human Genome Research Institute (UM1HG006504 and U24HG008956), the French National Research Agency under the “Investments for the Future” program (ANR-10-IAHU-01), the Integrative Biology of Emerging Infectious Diseases Laboratory of Excellence (ANR-10-LABX-62-IBEID), the French Foundation for Medical Research (EQU201903007798), the French Foundation for Medical Research and French National Research Agency GENCOVID project, ANRS-COV05, the Square Foundation, Grandir-Fonds de Solidarité pour l’Enfance, the SCOR Corporate Foundation for Science, Institut National de la Santé et de la Recherche Médicale, and the University of Paris. The work was supported in part by the Intramural Research Program of the National Institute of Allergy and Infectious Diseases, National Institutes of Health. J. Rosain is supported by the Institut National de la Santé et de la Recherche Médicale PhD program (“poste d’accueil Inserm”) and the MD-PhD program of the Imagine Institute (with the support of the Fondation Bettencourt Schueller). P. Bastard was supported by the French Foundation for Medical Research (EA20170638020). P. Bastard and T. Le Voyer were supported by the MD-PhD program of the Imagine Institute (with the support of the Fondation Bettencourt Schueller). Work in the Laboratory of Virology and Infectious Diseases at The Rockefeller University was supported by the National Institutes of Health, National Institute of Allergy and Infectious Diseases grant 1R01AI124690 (to C.M. Rice). The content is solely the responsibility of the authors and does not necessarily represent the official views of the any of the funding sources.

Author contributions: P. Bastard identified the auto-Abs in the three patients. P. Bastard and M. Chbihi identified the *IFNAR2* variant. P. Bastard, E. Michailidis, H.-H. Hoffmann, M. Chbihi, T. Le Voyer, J. Rosain, Q. Philippot, A. Gervais, M. Materna, L.V. Erazo, F. Rozenberg, M.M. Jeljeli, R. Yang, Y. Seeleuthner, L.B. Rosen, L. Lorenzo, L. Bizien, and M. Chrabieh performed experiments or generated and analyzed data. A.P. Dinis Ano Bom, D. Araújo da Conceição, B. Pulendran, R. Huits, A. Homma, M.d.L.S. Maia, T. Azamor, P.M.N. de Oliveira, J.D. Miller, E. Goudouris, R. Ahmed, S.J. Seligman, G. Slesak, and J. Schäfer recruited or treated the patients. V. Béziat, S.M. Holland, A. Cobat, L.D. Notarangelo, H.C. Su, L. Abel, A. Puel, S.-Y. Zhang, Q. Zhang, M.R. MacDonald, E. Jouanguy, C.M. Rice, and J.-L. Casanova supervised the experiments. M.R. MacDonald, E. Jouanguy, C.M. Rice, and J.-L. Casanova supervised the project. P. Bastard and J.-L. Casanova wrote the manuscript. All the authors edited the manuscript.

Disclosures: A. Homma reported, “Our institution is a non-profit producer of the yellow fever vaccine. We are public institution,

part of our Ministry of Health, and provide vaccine only for National Immunization Program and UNICEF, PAHO Revolving Fund, GAVI, and WHO. We are very much interested to know all relevant scientific issues involved with our vaccine.” J.L. Casanova reported a patent to application number 63/055,155, filed July 22, 2020 pending. No other disclosures were reported.

Submitted: 20 November 2020

Revised: 21 December 2020

Accepted: 19 January 2021

References

- Adzhubei, I.A., S. Schmidt, L. Peshkin, V.E. Ramensky, A. Gerasimova, P. Bork, A.S. Kondrashov, and S.R. Sunyaev. 2010. A method and server for predicting damaging missense mutations. *Nat. Methods*. 7:248–249. <https://doi.org/10.1038/nmeth0410-248>
- Bastard, P., J. Manry, J. Chen, J. Rosain, Y. Seeleuthner, O. AbuZaitun, L. Lorenzo, T. Khan, M. Hasek, N. Hernandez, et al. 2020a. Herpes simplex encephalitis in a patient with a distinctive form of inherited *IFNAR1* deficiency. *J. Clin. Invest.* 131:e139980. <https://doi.org/10.1172/JCI139980>
- Bastard, P., L.B. Rosen, Q. Zhang, E. Michailidis, H.H. Hoffmann, Y. Zhang, K. Dorgham, Q. Philippot, J. Rosain, V. Béziat, et al. 2020b. Autoantibodies against type I IFNs in patients with life-threatening COVID-19. *Science*. 370:eabd4585. <https://doi.org/10.1126/science.abd4585>
- Bousfiha, A., L. Jeddane, C. Picard, W. Al-Herz, F. Ailal, T. Chatila, C. Cunningham-Rundles, A. Etzioni, J.L. Franco, S.M. Holland, et al. 2020. Human Inborn Errors of Immunity: 2019 Update of the IUIS Phenotypical Classification. *J. Clin. Immunol.* 40:66–81. <https://doi.org/10.1007/s10875-020-00758-x>
- Bravo García-Morato, M., A. Calvo Apalategi, L.Y. Bravo-Gallego, A. Blázquez Moreno, M. Simón-Fuentes, J.V. Garmendia, A. Méndez Echevarría, T. Del Rosal Rabes, Á. Domínguez-Soto, E. López-Granados, et al. 2019. Impaired control of multiple viral infections in a family with complete *IRF9* deficiency. *J. Allergy Clin. Immunol.* 144:309–312.e10. <https://doi.org/10.1016/j.jaci.2019.02.019>
- Chan, R.C., D.J. Penney, D. Little, I.W. Carter, J.A. Roberts, and W.D. Rawlinson. 2001. Hepatitis and death following vaccination with 17D-204 yellow fever vaccine. *Lancet*. 358:121–122. [https://doi.org/10.1016/S0140-6736\(01\)05341-7](https://doi.org/10.1016/S0140-6736(01)05341-7)
- Duncan, C.J., S.M. Mohamad, D.F. Young, A.J. Skelton, T.R. Leahy, D.C. Munday, K.M. Butler, S. Morfopoulou, J.R. Brown, M. Hubank, et al. 2015. Human *IFNAR2* deficiency: Lessons for antiviral immunity. *Sci. Transl. Med.* 7:307ra154. <https://doi.org/10.1126/scitranslmed.aac4227>
- Dupuis, S., E. Jouanguy, S. Al-Hajjar, C. Fieschi, I.Z. Al-Mohsen, S. Al-Jumaah, K. Yang, A. Chapgier, C. Eidenschenk, P. Eid, et al. 2003. Impaired response to interferon-alpha/beta and lethal viral disease in human *STAT1* deficiency. *Nat. Genet.* 33:388–391. <https://doi.org/10.1038/ng1097>
- Eletto, D., S.O. Burns, I. Angulo, V. Plagnol, K.C. Gilmour, F. Henriquez, J. Curtis, M. Gaspar, K. Nowak, V. Daza-Cajigal, et al. 2016. Biallelic *JAK1* mutations in immunodeficient patient with mycobacterial infection. *Nat. Commun.* 7:13992. <https://doi.org/10.1038/ncomms13992>
- Gershman, M.D., J.E. Staples, A.D. Bentsi-Enchill, J.G. Breugelmanns, G.S. Brito, L.A. Camacho, P. Cottin, C. Domingo, A. Durbin, J. Gascon, et al. Brighton Collaboration Viscerotropic Disease Working Group. 2012. Viscerotropic disease: case definition and guidelines for collection, analysis, and presentation of immunization safety data. *Vaccine*. 30: 5038–5058. <https://doi.org/10.1016/j.vaccine.2012.04.067>
- Gothe, F., C.F. Hattori, L. Truong, Z. Klimova, V. Kanderova, M. Fejtкова, A. Grainger, V. Bigley, J. Perthen, D. Mitra, et al. 2020. A novel case of homozygous *IFNAR1* deficiency with haemophagocytic lymphohistiocytosis. *Clin. Infect. Dis.: ciaa1790*. <https://doi.org/10.1093/cid/ciaa1790>
- Gupta, S., I.P. Tatouli, L.B. Rosen, S. Hasni, I. Alevizos, Z.G. Manna, J. Rivera, C. Jiang, R.M. Siegel, S.M. Holland, et al. 2016. Distinct Functions of Autoantibodies Against Interferon in Systemic Lupus Erythematosus: A Comprehensive Analysis of Anticytokine Autoantibodies in Common Rheumatic Diseases. *Arthritis Rheumatol.* 68:1677–1687. <https://doi.org/10.1002/art.39607>
- Hambleton, S., S. Goodbourn, D.F. Young, P. Dickinson, S.M. Mohamad, M. Valappil, N. McGovern, A.J. Cant, S.J. Hackett, P. Ghazal, et al. 2013.

- STAT2 deficiency and susceptibility to viral illness in humans. *Proc. Natl. Acad. Sci. USA.* 110:3053–3058. <https://doi.org/10.1073/pnas.1220098110>
- Hernandez, N., I. Melki, H. Jing, T. Habib, S.S.Y. Huang, J. Danielson, T. Kula, S. Drutman, S. Belkaya, V. Rattina, et al. 2018. Life-threatening influenza pneumonitis in a child with inherited IRF9 deficiency. *J. Exp. Med.* 215:2567–2585. <https://doi.org/10.1084/jem.20180628>
- Hernandez, N., G. Bucciol, L. Moens, J. Le Pen, M. Shahrooei, E. Goudouris, A. Shirkami, M. Changi-Ashtiani, H. Rokni-Zadeh, E.H. Sayar, et al. 2019. Inherited IFNAR1 deficiency in otherwise healthy patients with adverse reaction to measles and yellow fever live vaccines. *J. Exp. Med.* 216:2057–2070. <https://doi.org/10.1084/jem.20182295>
- Howe, H.S., and B.P.L. Leung. 2019. Anti-Cytokine Autoantibodies in Systemic Lupus Erythematosus. *Cells.* 9:72. <https://doi.org/10.3390/cells9010072>
- Itan, Y., L. Shang, B. Boisson, M.J. Ciancanelli, J.G. Markle, R. Martinez-Barricarte, E. Scott, I. Shah, P.D. Stenson, J. Gleeson, et al. 2016. The mutation significance cutoff: gene-level thresholds for variant predictions. *Nat. Methods.* 13:109–110. <https://doi.org/10.1038/nmeth.3739>
- Kircher, M., D.M. Witten, P. Jain, B.J. O’Roak, G.M. Cooper, and J. Shendure. 2014. A general framework for estimating the relative pathogenicity of human genetic variants. *Nat. Genet.* 46:310–315. <https://doi.org/10.1038/ng.2892>
- Kreins, A.Y., M.J. Ciancanelli, S. Okada, X.F. Kong, N. Ramirez-Alejo, S.S. Kilic, J. El Baghdadi, S. Nonoyama, S.A. Mahdavian, F. Ailal, et al. 2015. Human TYK2 deficiency: Mycobacterial and viral infections without hyper-IgE syndrome. *J. Exp. Med.* 212:1641–1662. <https://doi.org/10.1084/jem.20140280>
- Ku, C.L., C.Y. Chi, H. von Bernuth, and R. Doffinger. 2020. Autoantibodies against cytokines: phenocopies of primary immunodeficiencies? *Hum. Genet.* 139:783–794. <https://doi.org/10.1007/s00439-020-02180-0>
- Lazear, H.M., J.W. Schoggins, and M.S. Diamond. 2019. Shared and Distinct Functions of Type I and Type III Interferons. *Immunity.* 50:907–923. <https://doi.org/10.1016/j.immuni.2019.03.025>
- Lecomte, E., G. Laureys, F. Verbeke, C. Domingo Carrasco, M. Van Esbroeck, and R. Huits. 2020. A clinician’s perspective on yellow fever vaccine-associated neurotropic disease. *J. Travel Med.* 27:taaa172. <https://doi.org/10.1093/jtm/taaa172>
- Li, H., and R. Durbin. 2009. Fast and accurate short read alignment with Burrows-Wheeler transform. *Bioinformatics.* 25:1754–1760. <https://doi.org/10.1093/bioinformatics/btp324>
- Li, H., B. Handsaker, A. Wysoker, T. Fennell, J. Ruan, N. Homer, G. Marth, G. Abecasis, and R. Durbin. 1000 Genome Project Data Processing Subgroup. 2009. The Sequence Alignment/Map format and SAMtools. *Bioinformatics.* 25:2078–2079. <https://doi.org/10.1093/bioinformatics/btp352>
- Lindsey, N.P., I.B. Rabe, E.R. Miller, M. Fischer, and J.E. Staples. 2016. Adverse event reports following yellow fever vaccination, 2007–13. *J. Travel Med.* 23:taw045. <https://doi.org/10.1093/jtm/taw045>
- Martin, M., T.F. Tsai, B. Cropp, G.J. Chang, D.A. Holmes, J. Tseng, W. Shieh, S.R. Zaki, I. Al-Sanouri, A.F. Cutrona, et al. 2001. Fever and multisystem organ failure associated with 17D-204 yellow fever vaccination: a report of four cases. *Lancet.* 358:98–104. [https://doi.org/10.1016/S0140-6736\(01\)05327-2](https://doi.org/10.1016/S0140-6736(01)05327-2)
- Martins, R.M., A.L. Pavão, P.M. de Oliveira, P.R. dos Santos, S.M. Carvalho, R. Mohrdieck, A.R. Fernandes, H.K. Sato, P.M. de Figueiredo, V.R. von Doellinger, et al. 2014. Adverse events following yellow fever immunization: Report and analysis of 67 neurological cases in Brazil. *Vaccine.* 32:6676–6682. <https://doi.org/10.1016/j.vaccine.2014.05.003>
- Mathian, A., S. Mouries-Martin, K. Dorgham, H. Devilliers, L. Barnabei, E. Ben Salah, F. Cohen-Aubart, L. Garrido Castillo, J. Haroche, M. Hie, et al. 2019. Monitoring Disease Activity in Systemic Lupus Erythematosus With Single-Molecule Array Digital Enzyme-Linked Immunosorbent Assay Quantification of Serum Interferon- α . *Arthritis Rheumatol.* 71:756–765. <https://doi.org/10.1002/art.40792>
- McKenna, A., M. Hanna, E. Banks, A. Sivachenko, K. Cibulskis, A. Kernytzky, K. Garimella, D. Altshuler, S. Gabriel, M. Daly, and M.A. DePristo. 2010. The Genome Analysis Toolkit: a MapReduce framework for analyzing next-generation DNA sequencing data. *Genome Res.* 20:1297–1303. <https://doi.org/10.1101/gr.107524.110>
- Meager, A., K. Visvalingam, P. Peterson, K. Möll, A. Murumägi, K. Krohn, P. Eskelin, J. Perheentupa, E. Husebye, Y. Kadota, and N. Willcox. 2006. Anti-interferon autoantibodies in autoimmune polyendocrinopathy syndrome type 1. *PLoS Med.* 3:e289. <https://doi.org/10.1371/journal.pmed.0030289>
- Monath, T.P. 2005. Yellow fever vaccine. *Expert Rev. Vaccines.* 4:553–574. <https://doi.org/10.1586/14760584.4.4.553>
- Monath, T.P., M.S. Cetron, K. McCarthy, R. Nichols, W.T. Archambault, L. Weld, and P. Bedford. 2005. Yellow fever 17D vaccine safety and immunogenicity in the elderly. *Hum. Vaccin.* 1:207–214. <https://doi.org/10.4161/hv.1.5.2221>
- Ng, P.C., and S. Henikoff. 2001. Predicting deleterious amino acid substitutions. *Genome Res.* 11:863–874. <https://doi.org/10.1101/gr.176601>
- Notarangelo, L.D., R. Bacchetta, J.L. Casanova, and H.C. Su. 2020. Human inborn errors of immunity: An expanding universe. *Sci. Immunol.* 5:eabb1662. <https://doi.org/10.1126/sciimmunol.abb1662>
- Panem, S., I.J. Check, D. Henriksen, and J. Vilcek. 1982. Antibodies to alpha-interferon in a patient with systemic lupus erythematosus. *J. Immunol.* 129:1–3.
- Pulendran, B., J. Miller, T.D. Querec, R. Akondy, N. Moseley, O. Laur, J. Glidewell, N. Monson, T. Zhu, H. Zhu, et al. 2008. Case of yellow fever vaccine-associated viscerotropic disease with prolonged viremia, robust adaptive immune responses, and polymorphisms in CCR5 and RANTES genes. *J. Infect. Dis.* 198:500–507. <https://doi.org/10.1086/590187>
- Russell-Harde, D., T.C. Wagner, M.R. Rani, D. Vogel, O. Colamonici, R.M. Ransohoff, B. Majchrzak, E. Fish, H.D. Perez, and E. Croze. 2000. Role of the intracellular domain of the human type I interferon receptor 2 chain (IFNAR2c) in interferon signaling. Expression of IFNAR2c truncation mutants in U5A cells. *J. Biol. Chem.* 275:23981–23985. <https://doi.org/10.1074/jbc.M002518200>
- Sanchez-Felipe, L., T. Vercruyse, S. Sharma, J. Ma, V. Lemmens, D. Van Looveren, M.P. Arkalagud Javarappa, R. Boudewijns, B. Malengier-Devlies, L. Liesenborghs, et al. 2020. A single-dose live-attenuated YF17D-vectored SARS-CoV-2 vaccine candidate. *Nature.* <https://doi.org/10.1038/s41586-020-3035-9>
- Seligman, S.J. 2014. Risk groups for yellow fever vaccine-associated viscerotropic disease (YEL-AVD). *Vaccine.* 32:5769–5775. <https://doi.org/10.1016/j.vaccine.2014.08.051>
- Seligman, S.J., and J.L. Casanova. 2016. Yellow fever vaccine: worthy friend or stealthy foe? *Expert Rev. Vaccines.* 15:681–691. <https://doi.org/10.1080/14760584.2016.1180250>
- Slesak, G., M. Gabriel, C. Domingo, and J. Schäfer. 2017. [Severe Yellow fever vaccine-associated disease: a case report and current overview]. *Dtsch. Med. Wochenschr.* 142:1219–1222. <https://doi.org/10.1055/s-0043-114729>
- Tangye, S.G., W. Al-Herz, A. Bousfiha, T. Chatila, C. Cunningham-Rundles, A. Etzioni, J.L. Franco, S.M. Holland, C. Klein, T. Morio, et al. 2020. Human Inborn Errors of Immunity: 2019 Update on the Classification from the International Union of Immunological Societies Expert Committee. *J. Clin. Immunol.* 40:24–64. <https://doi.org/10.1007/s10875-019-00737-x>
- Vasconcelos, P.F., E.J. Luna, R. Galler, L.J. Silva, T.L. Coimbra, V.L. Barros, T.P. Monath, S.G. Rodrigues, C. Laval, Z.G. Costa, et al. Brazilian Yellow Fever Vaccine Evaluation Group. 2001. Serious adverse events associated with yellow fever 17DD vaccine in Brazil: a report of two cases. *Lancet.* 358:91–97. [https://doi.org/10.1016/S0140-6736\(01\)05326-0](https://doi.org/10.1016/S0140-6736(01)05326-0)
- Walter, J.E., L.B. Rosen, K. Csomos, J.M. Rosenberg, D. Mathew, M. Keszei, B. Ujhazi, K. Chen, Y.N. Lee, I. Tirosh, et al. 2015. Broad-spectrum antibodies against self-antigens and cytokines in RAG deficiency. *J. Clin. Invest.* 125:4135–4148. <https://doi.org/10.1172/JCI80477>
- Watford, W.T., and J.J. O’Shea. 2006. Human tyk2 kinase deficiency: another primary immunodeficiency syndrome. *Immunity.* 25:695–697. <https://doi.org/10.1016/j.immuni.2006.10.007>
- Wilmes, S., O. Beutel, Z. Li, V. Francois-Newton, C.P. Richter, D. Janning, C. Kroll, P. Hanhart, K. Hötte, C. You, et al. 2015. Receptor dimerization dynamics as a regulatory valve for plasticity of type I interferon signaling. *J. Cell Biol.* 209:579–593. <https://doi.org/10.1083/jcb.201412049>
- Yi, Z., L. Sperzel, C. Nürnberg, P.J. Bredendiek, K.J. Lubick, S.M. Best, C.T. Stoyanov, L.M. Law, Z. Yuan, C.M. Rice, and M.R. MacDonald. 2011. Identification and characterization of the host protein DNAJC14 as a broadly active flavivirus replication modulator. *PLoS Pathog.* 7:e1001255. <https://doi.org/10.1371/journal.ppat.1001255>
- Zhang, Q., P. Bastard, A. Bolze, E. Jouanguy, S.Y. Zhang, A. Cobat, L.D. Notarangelo, H.C. Su, L. Abel, and J.L. Casanova. COVID Human Genetic Effort. 2020a. Life-Threatening COVID-19: Defective Interferons Unleash Excessive Inflammation. *Med (N Y).* 1:14–20. <https://doi.org/10.1016/j.medj.2020.12.001>
- Zhang, Q., P. Bastard, Z. Liu, J. Le Pen, M. Moncada-Velez, J. Chen, M. Ogishi, I.K.D. Sabli, S. Hodeib, C. Korol, et al. NIAID-USUHS/TAGC COVID Immunity Group. 2020b. Inborn errors of type I IFN immunity in patients with life-threatening COVID-19. *Science.* 370:eabd4570. <https://doi.org/10.1126/science.abd4570>

Supplemental material

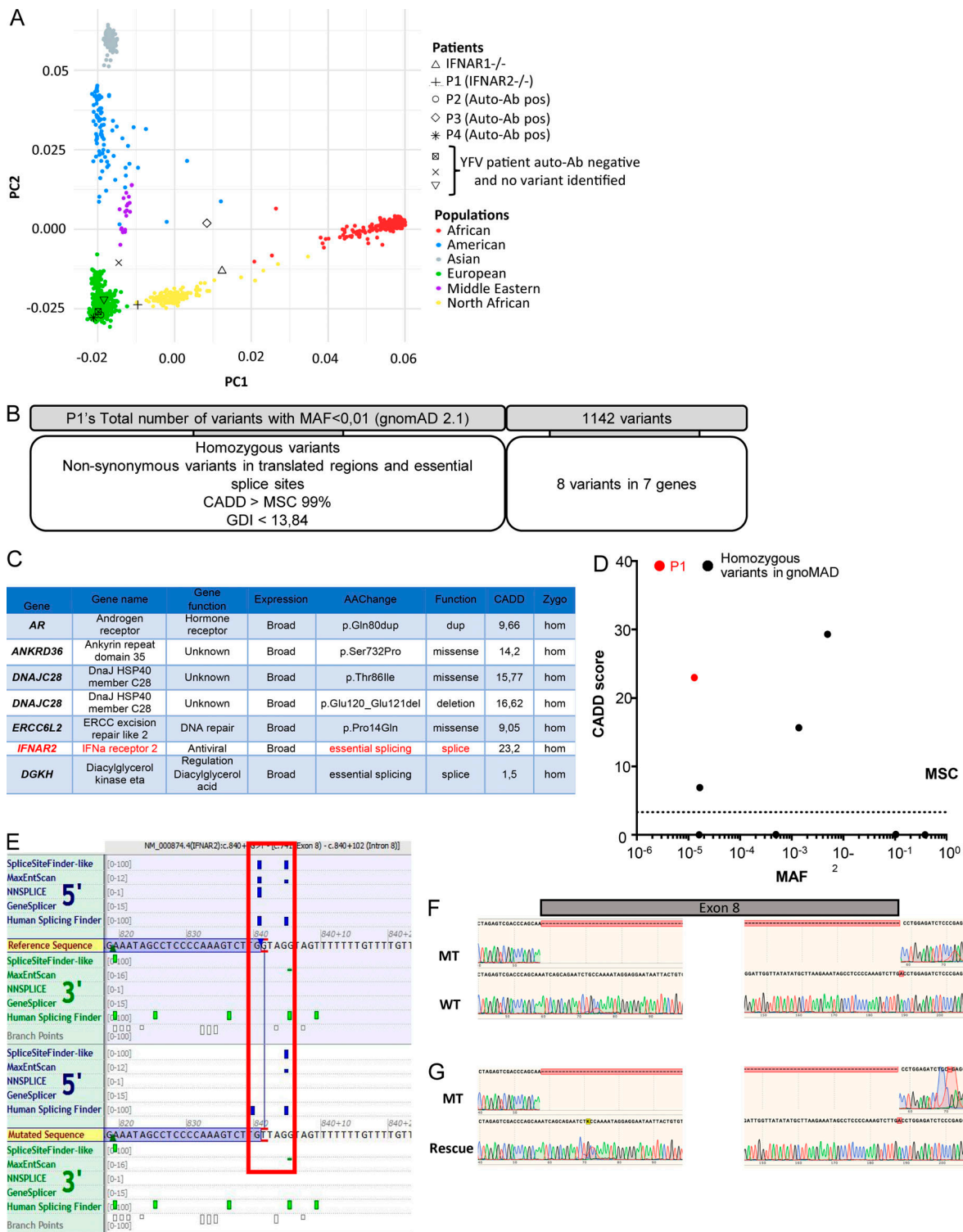


Figure S1. **Homozygous loss-of-function variant of *IFNAR2* in a patient with YEL-AVD.** (A) Principal component analysis (PCA) on the eight patients with life-threatening adverse reactions to YFV, including the patients with *IFNAR1* and *IFNAR2* deficiency, and those with auto-Abs against type I IFNs. (B) Filtering criteria used for the single-nucleotide variant analysis of whole-exome sequencing results for P1. (C) Single-nucleotide variants presented by the patient (P1) and meeting the filtering criteria, with the name, known function, and expression pattern of the gene. AACChange, amino acid change; Zygo, zygosity; Hom, homozygote; Dup, duplication. (D) Population genetics of homozygous coding missense *IFNAR2* variants present in gnomAD. No predicted loss-of-function variants are reported in gnomAD at the homozygous state. The patient's variant is shown in red, whereas the variants present in gnomAD are shown in black. CADD, combined annotation-dependent depletion; GDI, gene damage index; MSC, mutation significance cutoff. (E) Whole-exome sequencing results for the *IFNAR2* gene in P1, as shown in ALAMUT, at the end of exon 8. The predicted splicing effect of the variant is indicated with a red square. (F) Sequencing results demonstrating complete aberrant splicing of *IFNAR2* in the patient (MT) relative to the control (WT). (G) Sequencing results demonstrating normal splicing of *IFNAR2* in the patient (MT) when the gDNA variant is restored to the WT form (rescue). pos, positive.

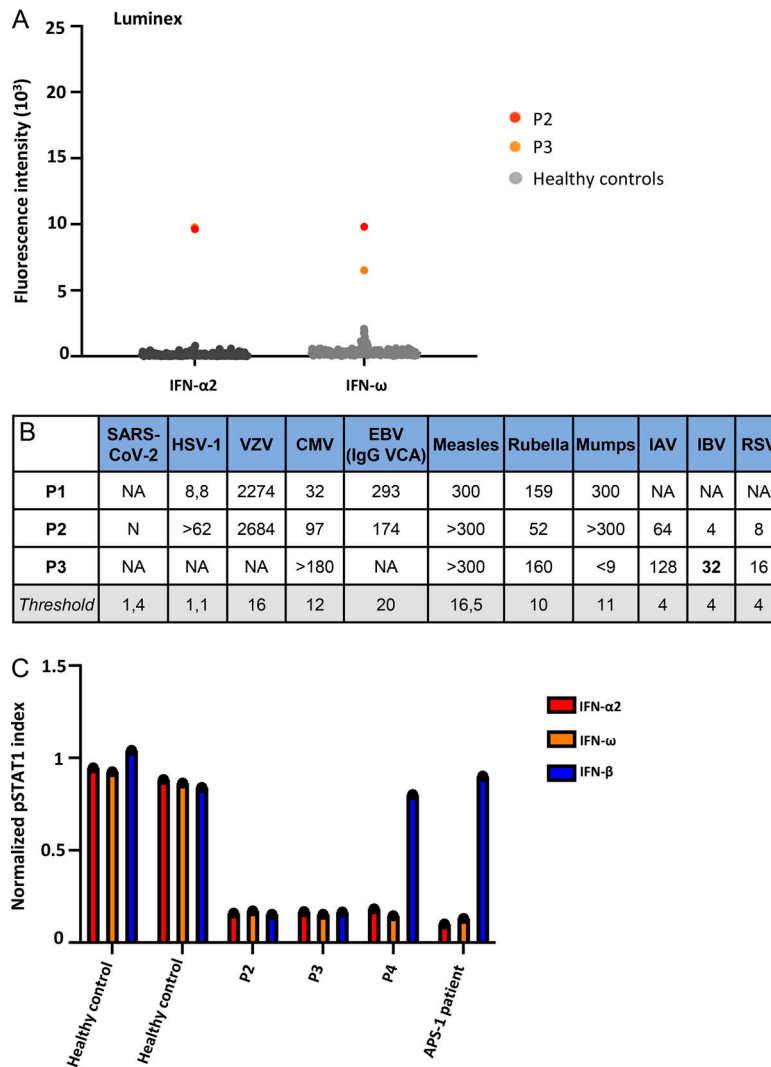


Figure S2. **Neutralizing auto-Abs against IFN- α 2 and IFN- ω in three patients with adverse reactions to yellow fever vaccine.** **(A)** Multiplex particle-based assay for auto-Abs against IFN- α 2 and IFN- ω in two patients with life-threatening adverse reactions to yellow fever vaccine and healthy controls ($n = 250$; previously used in Bastard et al., 2020b). **(B)** Serological data for IgG Abs against various viruses, for P1, P2, and P3. The threshold value for each viral serological test is indicated. N, negative; NA, not available. In serological tests for EBV, we measured anti-VCA (viral capsid antigen) Ab levels. HSV-1, herpes simplex virus 1; VZV, varicella zoster virus; CMV, cytomegalovirus; IAV, influenza A virus; IBV, Influenza B virus; RSV, respiratory syncytial virus. **(C)** Normalized pSTAT1 index based on fluorescence-activated cell sorting for IFN- α 2-, IFN- β -, or IFN- ω -induced pSTAT1 in healthy control cells in the presence of 10% healthy control plasma, or anti-IFN- α 2, anti-IFN- β , or anti-IFN- ω auto-Ab-containing plasma from YFV patients.

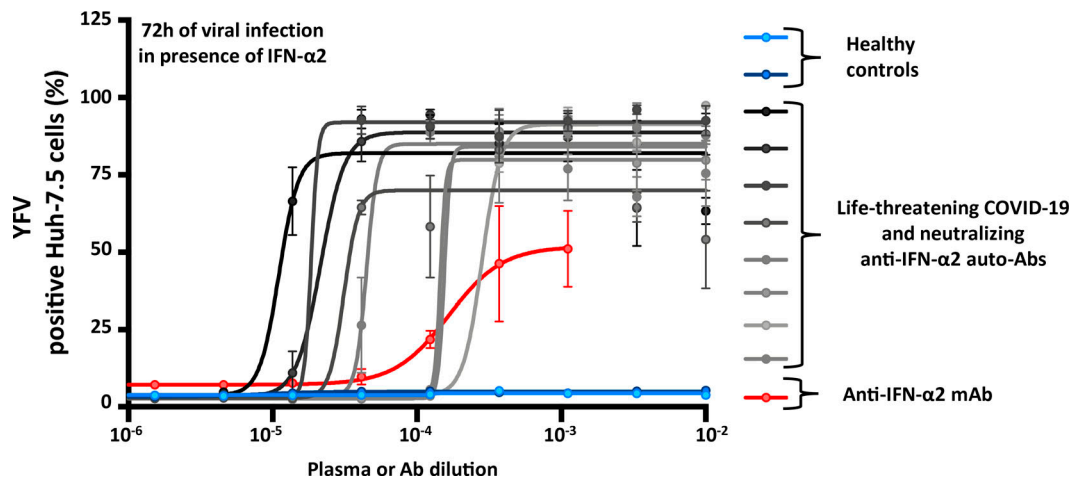


Figure S3. **Enhanced YFV replication, despite the presence of IFN-α2, in the presence of plasma from patients with life-threatening COVID-19 and auto-Abs against IFN-α2.** (A) YFV-17D replication, assessed 72 h after infection, in Huh-7.5 cells treated with IFN-α2, and in the presence of either plasma from patients with life-threatening COVID-19 and neutralizing auto-Abs against IFN-α2 ($n = 8$), or a commercial anti-IFN-α2 Ab, or plasma from healthy controls ($n = 2$). Error bars represent SEM.

Table S1, which is provided online, shows auto-Abs against other targets, used in clinical practice in two patients positive for auto-Abs to type I IFNs (P2 and P3).